



CHORUS

This is the accepted manuscript made available via CHORUS. The article has been published as:

Experimental thermal equation of state of $B_{2m}KCl$

B. A. Chidester, E. C. Thompson, R. A. Fischer, D. L. Heinz, V. B. Prakapenka, Y. Meng, and
A. J. Campbell

Phys. Rev. B **104**, 094107 — Published 22 September 2021

DOI: [10.1103/PhysRevB.104.094107](https://doi.org/10.1103/PhysRevB.104.094107)

1 **An experimental thermal equation of state of B2-KCl**

2 B. A. Chidester^{1,*}, E. C. Thompson², R. A. Fischer³, D. L.
3 Heinz¹, V. B. Prakapenka⁴, Y. Meng⁵ and A. J. Campbell¹

4 *¹Department of Geophysical Sciences,*

5 *University of Chicago, Chicago, IL 60637*

6 *²Department of Earth and Environmental Systems,*

7 *Sewanee: The University of the South, Sewanee, TN 37375*

8 *³Department of Earth and Planetary Sciences,*

9 *Harvard University, Cambridge, MA 02138*

10 *⁴Center for Advanced Radiation Sources,*

11 *University of Chicago, Chicago, IL 60439*

12 *⁵HPCAT, X-ray Science Division, Argonne National Laboratory, Lemont IL 60439 and*

13 **Present address: Los Alamos National Laboratory, bchides@lanl.gov*

14 (Dated: September 8, 2021)

Abstract

15

16 The alkali halides are often used as optically-transparent pressure-transmitting media and ther-
17 mal insulators in laser-heated diamond anvil cell experiments. High P - T equations of state for
18 these materials would allow them to be used simultaneously as sensitive *in situ* pressure markers,
19 making sample preparation and data analysis simpler. KCl is especially useful for this application
20 because its high melting point, crystallographic simplicity, and low electron density are ideal for use
21 in high-temperature X-ray diffraction experiments. However, the high-temperature static equation
22 of state data for this material is limited in pressure to 8 GPa. As experiments routinely exceed
23 100 GPa in pressure and thousands of Kelvin, it is necessary for the equation of state of KCl to be
24 determined experimentally at these conditions if it is to be used as an equation of state calibrant
25 in the future. This work combines new high-pressure, high-temperature data of the B2 phase of
26 KCl (up to 167 GPa and 2400 K) with the previously published room-temperature data of Dewaele
27 et al. (2012) to produce a Mie-Grüneisen-Debye thermal equation of state for this material. The
28 room temperature equation of state parameters are similar to those reported previously: $V_0 =$
29 $32.0(3)$ cm³/mole, $K_0 = 24(1)$ GPa and $K'_0 = 4.56(5)$. The thermal parameters, γ_0 and q , are
30 $2.9(4)$ and $1.0(1)$, respectively. While a q of 1 is expected, the γ_0 is higher than expected from
31 previous calculations, lower pressure experimental data, and the available shockwave data. Thus,
32 previously-reported equations of state underestimate the pressure of KCl at high temperatures.

33 I. INTRODUCTION

34 Alkali halides are simple ionic solids that have been studied under a wide variety of con-
35 ditions, making them useful benchmark materials to compare between dynamic and static
36 compressional environments. Additionally, their crystallographic simplicity and relatively
37 high compressibilities ($K_0 = \sim 10\text{--}30$ GPa) make them useful as pressure-transmitting me-
38 dia and potentially sensitive pressure markers in high-pressure X-ray diffraction (XRD)
39 experiments.¹ Furthermore, they are chemically inert and are transparent to near-infrared
40 light, which facilitates their use in high-temperature experiments, such as laser heating in a
41 diamond anvil cell (LH-DAC). Potassium chloride (KCl) has a higher melting point at high
42 pressures than NaCl or LiF,² but is less electronically dense than KBr or CsI, making it op-
43 timal among alkali halides as a pressure medium, pressure standard, and thermal insulator
44 for this type of high pressure-temperature (P - T) XRD experiment.

45 The room temperature phase behavior and equations of state of KCl have been investi-
46 gated up to 165 GPa.³⁻⁶ Early studies of KCl in the diamond anvil cell at room temperature
47 were conducted without the benefit of a (quasi)-hydrostatic pressure medium,³⁻⁵ and the
48 only high-temperature study of this material was limited to 8 GPa and 873 K.⁷ More re-
49 cently, Dewaele et al. (2012)⁶ has extended the room temperature data to 165 GPa under
50 hydrostatic conditions using He as the pressure medium and ruby as the pressure standard.
51 Similar to other alkali halides, KCl exhibits the NaCl (B1, $Fm\bar{3}m$) crystal structure at am-
52 bient conditions, and transforms to the CsCl (B2, $Pm\bar{3}m$) structure around 2 GPa at room
53 temperature.⁷ No other solid phase transitions of this material have been observed up to
54 165 GPa at room temperature, nor is one expected at high temperatures in this pressure
55 range.⁶

56 As high P - T experiments in the laser-heated diamond anvil cell routinely push conditions
57 to pressures above 100 GPa and temperatures of several thousand K, a high-temperature,
58 high-pressure equation of state of KCl is necessary to use this material as a pressure standard
59 for this type of experiment. In addition to high-pressure, room-temperature experiments,
60 Dewaele et al.⁶ performed molecular dynamics simulations to generate a constant thermal
61 pressure coefficient, $\alpha K_T = 0.00224$ GPa/K. This value is similar to the thermal pressure
62 coefficient experimentally measured between room temperature and 873 K by Ref. 7, 0.00275
63 GPa/K, while both of these coefficients are slightly lower than the constant $\alpha K_T = 0.0036$

64 GPa/K that can be calculated assuming a constant $C_V = 3nR$ (where n is the number of
65 elements per mole of KCl and R is the ideal gas constant) from the Grüneisen parameter,
66 $\gamma = 2.30$, derived from acoustic wave velocity measurements.⁸ A more accurate equation
67 of state requires experimental data to be obtained over a greater range of simultaneous
68 high-temperature, high-pressure conditions. This study combines new high pressure-volume-
69 temperature P - V - T synchrotron XRD data for KCl up to 167 GPa and 2400 K with previous
70 high-pressure, room-temperature data⁶ toward the aim of making KCl a useful and reliable
71 pressure standard for future high-pressure experiments.

72 II. METHODS

73 KCl (reagent grade) and Pt (99.9+%, 325 mesh) were purchased from Alfa Aesar. To
74 remove adsorbed moisture, the KCl was baked at ~ 100 °C for 12–24 hours prior to sample
75 preparation. Generally, LH-DAC samples consist of a thin foil of opaque sample material
76 encased between layers of a soft, transparent material that acts as both the thermal insulator
77 and as the quasi-hydrostatic pressure medium for the experiment. It is possible to use the
78 pressure medium/thermal insulator as an internal pressure calibrant as well (see Campbell
79 et al. (2009)⁹, for example). Thus, the samples in this study were configured to produce an
80 equation of state of KCl specifically for use as a pressure standard in this type of sample
81 geometry. Here, platinum (Pt) metal was used as the pressure calibrant and laser-absorbing
82 foil. Pt foils of ~ 5 μm thickness were secured between two layers of dried KCl of ~ 10 μm
83 thickness. Samples were loaded into diamond anvil cells using Re as the gasket material and
84 diamond culets of 300, 150 or 100 μm in diameter. The entire cell assembly was then dried
85 at 100 °C for ≥ 30 minutes to ensure total removal of moisture immediately prior to closing
86 and pressurizing the cell. (P - V - T) data were collected by compressing to a target pressure
87 and collecting powder XRD patterns at increasing (and/or decreasing) temperatures during
88 laser heating.

89 Angle-dispersive synchrotron X-ray diffraction (Fig. 1) was conducted at beamlines 13-ID-
90 D (GSE-CARS) and 16-ID-B (HP-CAT) of the Advanced Photon Source, Argonne National
91 Laboratory. Laser-heating experiments at beamline 13-ID-D were done with monochromatic
92 incident radiation ($\lambda = 0.3344$ or 0.2952 Å) measuring 2.2 by 4 μm .¹⁰ Laser-heating experi-
93 ments at beamline 16-ID-B were done with monochromatic incident radiation ($\lambda = 0.4066$

94 Å) measuring 6 by 7.5 μm .¹¹ Sample-to-detector distances and tilt were calibrated using
95 LaB₆ or CeO₂. The laser was co-aligned with the incident X-rays using the X-ray-induced
96 fluorescence of KCl. Double-sided laser-heating of the samples was performed using 1 μm
97 Yb-doped fiber lasers, adjusting upstream and downstream laser powers to balance tem-
98 peratures. The highest pressure measurements (sample B86) were conducted using “burst”
99 mode, where the lasers were enabled at the desired laser power only during XRD collection
100 to minimize accumulated heating of the DAC. This allowed the DAC to stay cool enough
101 that the laser-to-X-ray alignment was maintained throughout the entire heating cycle. Sur-
102 face temperatures were determined spectroradiometrically on both sides using the greybody
103 approximation,^{10,11} which were then corrected by -3% for a small axial temperature gradi-
104 ent across the metal to determine the average temperature of the Pt foil.^{9,12} The average
105 KCl temperature was taken as the temperature at the midpoint between the surface of the
106 sample and the surface of the diamond anvils; thus, the estimated average temperature of
107 the KCl pressure medium is $T_{KCl} = (3 * T_{surface} + 295) / 4 \pm (T_{surface} - 295) / 4$.⁹ Although
108 this geometry places a large uncertainty on the KCl temperature, this material remains an
109 effective pressure calibrant because the compressibility of alkali halides far outweighs their
110 thermal expansion over typical P - T conditions.⁹

111 Powder X-ray diffraction patterns were collected on a CCD image plate and integrated
112 azimuthally to intensity vs. 2θ plots (e.g. Fig. 1) using DIOPTAS.¹³ Reflection positions
113 were fit to determine lattice parameters as a function of pressure and temperature using
114 PeakFit (Systat Software). 2 to 7 reflections (110, 200, 211, 220, 310, 321, 222) were averaged
115 to determine the lattice parameters of KCl. Above 45 GPa, the KCl 200 reflection broadened
116 and yielded systematically-higher lattice parameters than all other lines (Fig. 2), so it was
117 not used in the volume calculation in that pressure range. Indeed, the 200 peak broadened
118 so significantly that it was lost in the background above 130 GPa. This phenomenon has
119 been observed previously in KCl⁶ and gold¹⁴, and was attributed to sensitivity of the 200
120 peak to non-hydrostatic strain. Pressure in these experiments was measured using the high
121 P - T equation of state of Pt¹⁵ and 3-8 observed reflections (111, 200, 220, 311, 222, 400, 331,
122 and 420). Note the non-hydrostatic behavior of the 200 reflection was not observed in the
123 Pt. The Pt equation of state¹⁵ is well-calibrated against the same pressure standards used
124 for the room-temperature KCl data.⁶

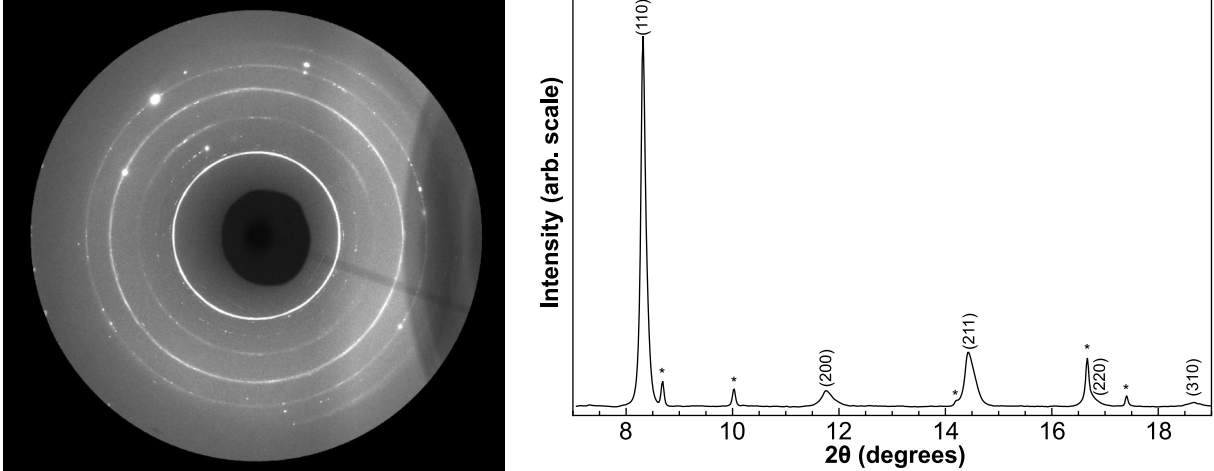


FIG. 1. Left: A typical XRD pattern from this study collected with X-ray wavelength $\lambda = 0.3344 \text{ \AA}$. Right: The integration of intensity vs. 2θ of the pattern on the left. The asterisks indicate reflections from the Pt pressure standard, while the KCl reflections are noted with their respective Miller indices (hkl). This pattern was collected at $31.8 \pm 0.9 \text{ GPa}$ and $1200 \pm 100 \text{ K}$ (Pt temperature).

125 III. THERMAL EQUATION OF STATE

126 The thermal equation of state (EOS) of B2-KCl was determined at high pressures and
 127 temperatures for use as a pressure standard in high P - T XRD experiments in the diamond
 128 anvil cell. The measured P - V - T data from four experiments are listed in Table A1.¹⁶ Fig.
 129 1 shows a sample diffraction pattern from this study at 31.6 GPa and 1194 K. As expected,
 130 the powder diffraction patterns became more “spotty,” as opposed to uniformly-defined
 131 rings, as temperatures increased. This is due to recrystallization and grain growth at high
 132 temperature and was more apparent in Pt than in KCl. The KCl peaks tended to be broad
 133 because the X-rays are sampling KCl at a range of temperatures between the Pt surface
 134 and the diamond culet. In most cases, data were obtained during cooling because the peak
 135 temperatures in each heating cycle significantly relaxed the sample and reduced lattice strain
 136 within the KCl. Recent observations of KBr in similar LH-DAC experiments suggest that
 137 this material will become opaque near its melting point, resulting in runaway heating and a
 138 miscalculation of its temperature.¹⁷ It is unclear whether this behavior occurs in other alkali
 139 halides; however, when runaway heating did occur at any point in an experiment, we only
 140 used data prior to that event to avoid inaccurate temperatures in our data. All experiments

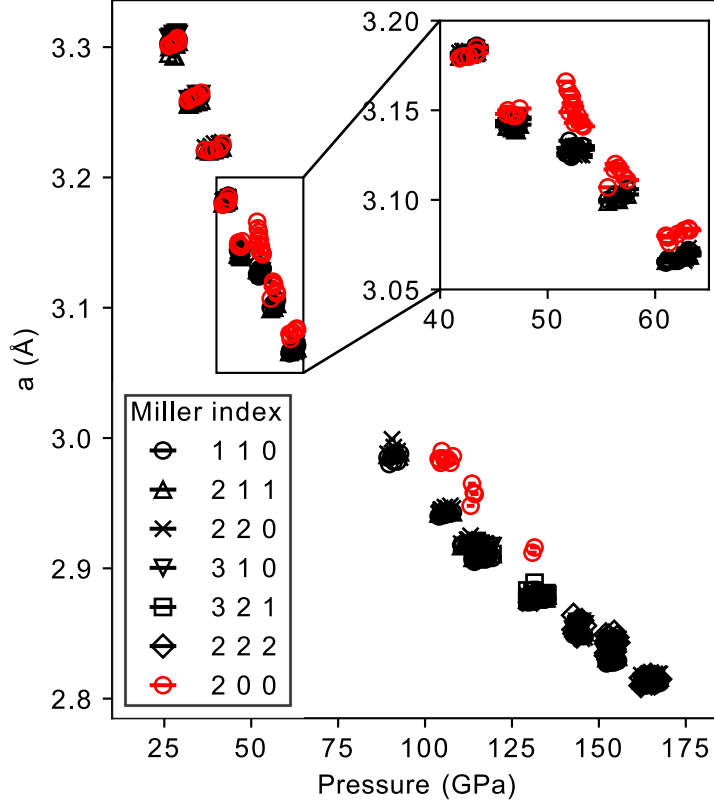


FIG. 2. Lattice parameter (a) for KCl from different XRD reflections. Above 50 GPa, the 200 reflection yields higher lattice parameters than all other reflections, so it was not used in the volume calculation in this pressure range. Above 130 GPa, the 200 peak cannot be distinguished from the background. Inset shows a blow-up of the 40-65 GPa range.

141 in this study were conducted above 15 GPa to stabilize and protect the diamonds during
 142 laser heating. This is well above the B1-to-B2 phase transition in KCl, reported at ~ 2 GPa.⁷
 143 No other phase transitions were observed up to 167 GPa and 2400 K in this study. Sample
 144 #2 was measured at both sector 13-ID-D and sector 16-ID-B. There was no distinguishable
 145 difference between these data.

146 We fit the high temperature data of B2 KCl, along with the room temperature data
 147 reported by Dewaele et al.,⁶ to a Mie-Grüneisen-Debye (M-G-D) thermal equation of state,
 148 defined as:

$$P = P_{300} + P_{thermal}, \quad (1)$$

149 where the room temperature data are described by:

$$P_{300,BM} = 3K_0 f(1 + 2f)^{\frac{5}{2}} \left(1 + \frac{3}{2}(K'_0 - 4)f\right). \quad (2)$$

150 Here, $P_{300,BM}$ is the Birch-Murnaghan¹⁸ isothermal equation of state at 300 K, f is the Eu-
 151 lerian strain ($\frac{1}{2}((\frac{V}{V_0})^{\frac{2}{3}} - 1)$), V_0 is the inferred zero-pressure volume of the B2 phase, K_0 and
 152 K'_0 are the isothermal zero-pressure bulk modulus and its pressure derivative, respectively.

153 Interestingly, while Dewaele et al.⁶ chose the Rydberg-Vinet (R-V) functional form for
 154 their isothermal equation of state, we found that a Birch-Murnaghan (B-M) EOS better
 155 describes their room temperature data, particularly at low pressures near the B1–B2 transi-
 156 tion. With the R-V fit, the lower-pressure, room-temperature residuals exhibit a monotonic
 157 trend with pressure, which the authors attributed to the B1–B2 phase transition affecting
 158 the bulk modulus of the B2 phase. This led them to fit only their lowest pressure data (2–6
 159 GPa) to determine V_0 . We find that when we fit the data to the B-M EOS, the residuals
 160 do not show such a trend with pressure and a reasonable, albeit slightly higher, V_0 can be
 161 inferred by fitting all of the B2-KCl data simultaneously. The resulting parameters for the
 162 calculated equations of state are given in Table 1, along with the thermal EOS parameters
 163 available in the literature. In terms of the room temperature B-M EOS, our fit agrees well
 164 with the literature data. The inferred zero-pressure volume, $V_0 = 32.0(3)$ cm³/mole, is the
 165 same as reported by both Refs. 5 and 7, within uncertainty. The bulk modulus, $K_0 = 24(1)$
 166 GPa, is very similar to that reported by Ref. 7, but lower than the 28.7 GPa reported by
 167 Ref. 5. This discrepancy is likely due to the fact that those authors chose to fix the pressure
 168 derivative of the bulk modulus, K'_0 , to 4. The larger pressure range sampled in Ref. 6
 169 allowed us to fit this parameter to 4.56(5). There is a trade-off between the fitted V_0 and
 170 K'_0 with K_0 , which is especially pronounced when comparing B-M and R-V-type fits; higher
 171 fitted V_0 values correspond to higher compressibility and a high change in compressibility
 172 with pressure. The room temperature equation of state fitting is demonstrated in Fig. 3,
 173 along with the data from Ref. 6 for reference.

174 The thermal contribution to pressure, $P_{thermal}$, is described by:

$$P_{thermal} = \frac{\gamma}{V} \times (E_{harmonic, T} - E_{harmonic, 300 K}), \quad (3)$$

175 and

TABLE I. Fitted equation of state parameters. Asterisks indicate parameters that were held constant during fitting. The γ_0 from Refs. 6 and 7 were calculated from the provided αK_T by assuming $\frac{V}{C_V}$ was constant. Values in parentheses are errors on the last digit. B-M is Burch-Murnaghan, R-V is Rydberg-Vinet.

V_0 (cm ³ /mole)	K_0 (GPa)	K'_0	γ_0	q	Reference (type of fit)
32.0(3)	24(1)	4.56(5)	2.9(4)	1.0(1)	This study (B-M reference EOS)
34.3(5)	13(1)	6.2(1)	3.4(4)	1.0(1)	This study (R-V reference EOS)
32.8*	17.2	5.89	1.47	1*	Ref. 6 (R-V)
32.25	23.7	4.4	1.78	1*	Ref. 7 (B-M)
31.83	28.7	4*	2.3	1*	Ref. 5 (B-M) + Ref. 8 (acoustic)

$$E_{\text{harmonic}} = 9nRT \left(\frac{T}{\theta_D}\right)^3 \int_0^{\theta_D/T} \frac{x^3}{e^x - 1} dx. \quad (4)$$

176 $\gamma = \gamma_0 \left(\frac{V}{V_0}\right)^q$ is the Grüneisen parameter, q is a constant, V is the volume, E_{harmonic} is the
177 harmonic contribution to thermal pressure at temperature, T , n is the number of atoms
178 per mole of KCl (2), R is the ideal gas constant and θ_D is the ambient-pressure Debye
179 temperature, 235 K.⁸

180 Instead of fitting a constant thermal pressure term (αK_T), we fit our data to the Debye
181 energy (Eq. 4), because at high pressures the Debye temperature is expected to exceed its
182 value at room temperature, such that the product αK_T is unlikely to be well approximated
183 as a constant.⁵ The thermal parameters, γ_0 and q , that describe our data are 2.9(4) and
184 1.0(1), respectively. The high-temperature data are also presented in Fig. 3, color-coded by
185 median temperature and plotted with their corresponding isotherms. The root-mean-square
186 misfit to the data over the whole pressure and temperature range is ± 1.6 GPa. The region of
187 largest error falls between 40 and 100 GPa, as shown in the residuals plot in Fig. 3. In this
188 pressure range, the two largest XRD peaks in the high-temperature data, the 110 of KCl and
189 the 111 of Pt, cross in 2θ space. We attribute the misfit in pressure to the high-temperature
190 data in this range to variations in calculated volume as a result of slight overlaps of these
191 two peaks.

192 Our fitted q value of 1.0(1) is typical and means that the Grüneisen parameter varies
193 proportional to volume. The fitted value of γ_0 is higher than expected based on both previous

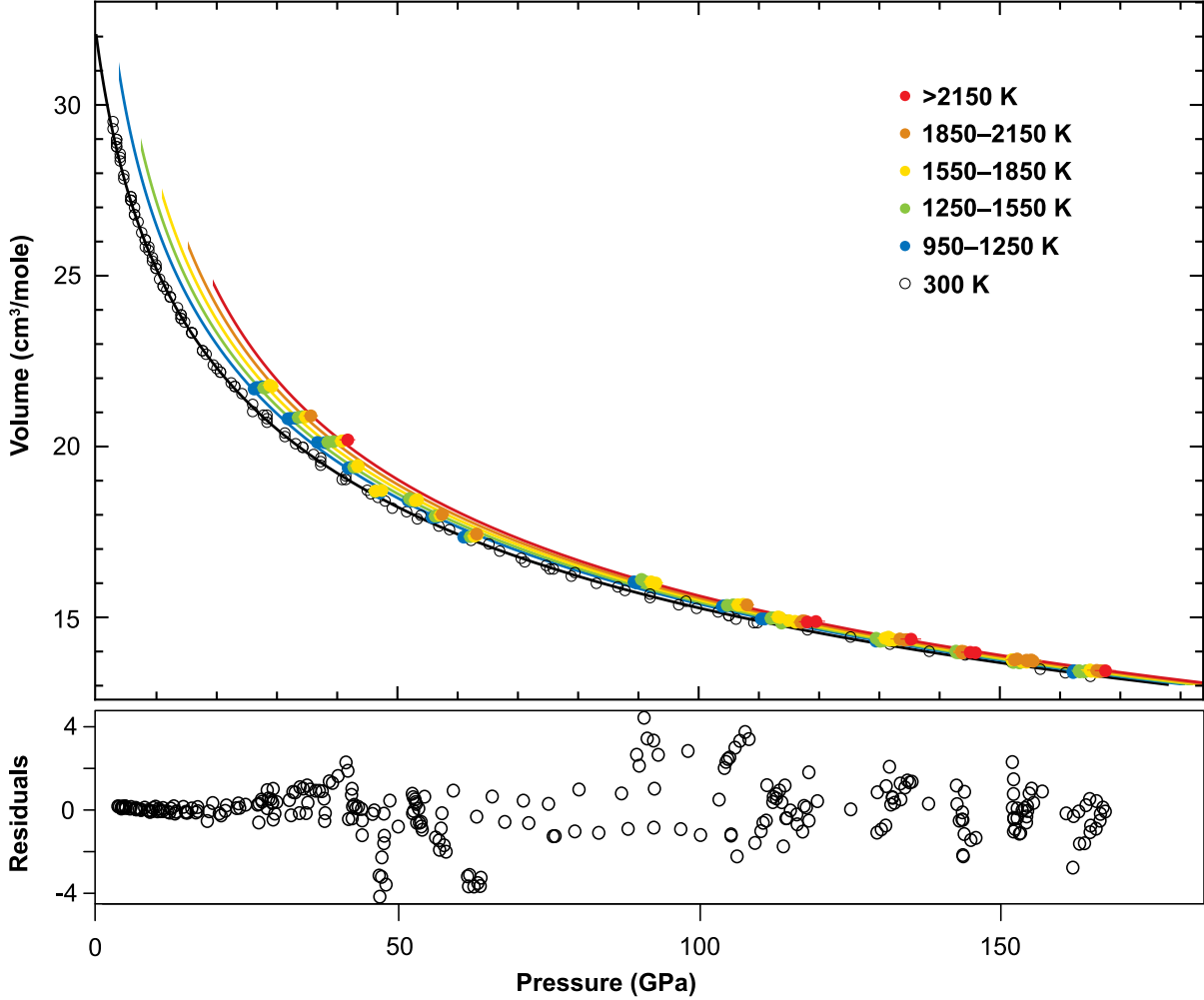


FIG. 3. Top: High P - T KCl data. Open black circles are room temperature data from Dewaele et al. (2012).⁶ High temperature data are color-coded by median temperature. Solid curves are isotherms calculated from the B-M equation of state parameters in Table 1. Error on volume is smaller than the symbol. Bottom: Residuals in pressure to the fit of all the data (300 K and room temperature).

194 static experiments and the available shockwave data.¹⁹ By assuming q is 1 and C_V is equal
 195 to the Debye limit, $3nR$, the value of γ_0 can be solved for based on the published parameters
 196 of Refs. 6 and 7 to be 1.47 and 1.78, respectively, using the relationship $\frac{\gamma}{V} = \frac{\gamma_0}{V_0} = \frac{\alpha K_T}{C_V}$. The
 197 thermal parameters in Ref. 6 were obtained from high-temperature molecular dynamics
 198 simulations, not experiments. Additionally, the data in Ref. 7 were measured only up to 8
 199 GPa and <1000 K, and one should not expect those results to be well-extrapolated over the
 200 much wider P - T range covered here. The γ_0 value measured acoustically in Ref. 8 is closer

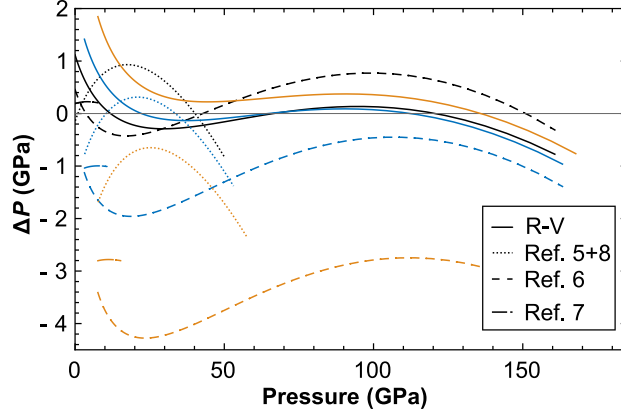


FIG. 4. Differences in calculated equations of state, $\Delta P = P - P_{\text{Birch-Murnaghan}}$ (*This study*), as a function of pressure. Black curves are calculated at 300 K, blue at 1000 K and gold at 2000 K. Different studies are represented by different dash formatting and are noted on the plot. Curves are plotted over the range of volume measured in each study. R-V = Rydberg-Vinet fit from this study.

201 to our value, at 2.3, but that study was also limited in pressure and temperature. Figure 4
 202 shows the comparison between the thermal equations of state reported in the literature and
 203 our fit up to 170 GPa. The R-V fit from this study generally matches our B-M EOS to \pm
 204 1 GPa, but overestimates the pressure slightly at low pressures and high temperatures. All
 205 of the thermal EOSs available in the literature do a reasonable job reproducing the data at
 206 room temperature, but underestimate the pressure at high temperatures by as much as 4
 207 GPa at 2000 K.

208 Figure 5 shows the 300 K isotherm resulting from this study, along with the principal
 209 isentrope and the principal shock Hugoniot calculated using our thermal equation of state
 210 and equation 5.

$$P_H = \frac{\frac{V}{\gamma} P_S + \int_{V_0}^V P_S dV - \Delta E_{\text{tr}}}{\frac{V}{\gamma} - \frac{V_{00} - V}{2}}. \quad (5)$$

211 P_H is the Hugoniot pressure, P_S is the principal isentropic compression curve, ΔE_{tr} is the
 212 change in energy due to the B1–B2 phase transition (31.4 J/mole)⁸, and V_{00} is the ambient
 213 pressure volume of the B1 phase (37.55 cm³/mole)⁶. The available shockwave data from
 214 Ref. 19 are also included in Fig. 5. It is clear that our predicted Hugoniot overestimates the
 215 pressure when compared with the shockwave data, corresponding to the higher Grüneisen

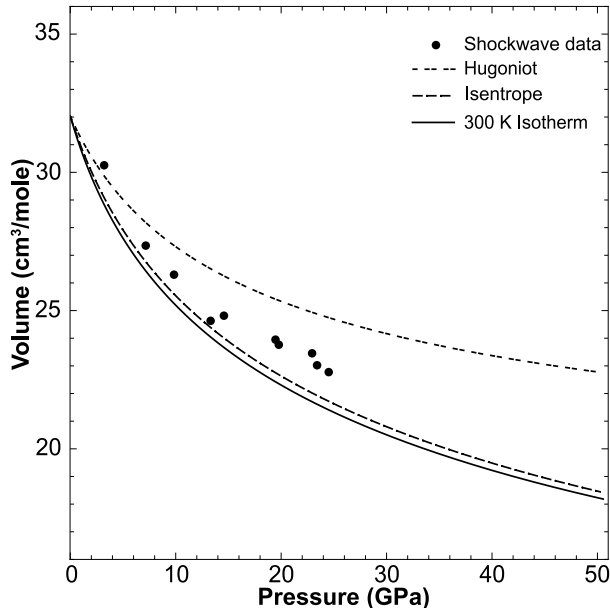


FIG. 5. The 300 K isotherm, principal isentrope and Hugoniot curves for KCl calculated from the high-temperature EOS. The measured shockwave data are shown for comparison. The B2 data end at ~ 25 GPa, at which point the material melts on the Hugoniot.

216 parameter in our equation of state. The shock wave data are better described using a γ_0
 217 of 1.6 to 1.7, depending on the reference equation of state used. These values are more
 218 compatible with those in Refs. 6 and 7. However, Ref. 8 reported a similar discrepancy to
 219 the one observed here between the γ_0 measured statically and the one extracted from the
 220 shockwave data. While the root cause of this discrepancy is unclear, possible causes may be
 221 differences in sample configuration or contamination of any of the samples by water.

223 IV. CONCLUSIONS

224 We have measured high P - T synchrotron X-ray diffraction on KCl in the laser-heated
 225 diamond anvil cell. These data, combined with the room temperature data from Ref. 6, were
 226 used to determine the Mie-Grüneisen-Debye equation of state for B2 KCl. The 300 K Birch-
 227 Murnaghan equation of state parameters measured here are very similar to those reported
 228 in the literature. There is a marked trade-off between the inferred V_0 term and the com-
 229 pressibility, which is exceptionally noticeable when comparing between Birch-Murnaghan
 230 and Rydberg-Vinet type fits. The thermal parameters, γ_0 and q , for KCl were found to be

231 2.9(4) and 1.0(1), respectively. This γ_0 value is higher than expected based on the calcu-
232 lations from Ref. 6 and the available shockwave data from Ref. 19, but is consistent with
233 that measured acoustically by Ref. 8. The measurements here extend the available data to
234 >100 GPa and several thousand degrees Kelvin. This greatly-expanded dataset has made a
235 more robust high P - T equation of state possible, which will allow KCl to be used as an *in*
236 *situ* pressure standard for high pressure-temperature XRD experiments in the laser-heated
237 diamond anvil cell.

238 ACKNOWLEDGMENTS

239 B.A.C. thanks D.M. Reaman, J. Britz and G. Myers for help with data collection. We
240 thank J.S. Pigott for use of his beamtime at HP-CAT. This work was funded by a NSF
241 Graduate Research Fellowship Grant #DGE-1144082 to B.A.C., NSF Postdoctoral Fellow-
242 ship EAR-1725673 to E.C.T., the Ludo Frevel Crystallography Scholarship from the In-
243 ternational Centre for Diffraction Data and the Postdoctoral Fellowship from the National
244 Science Foundation (EAR-1452626) to RAF, and NSF Grant #EAR-1427123 to A.J.C.
245 Parts of this work were conducted at HPCAT (Sector 16) and GeoSoilEnviroCARS (Sector
246 13), Advanced Photon Source (APS), Argonne National Laboratory. HPCAT operations
247 are supported by DOE-NNSA under Award #DE-NA0001974 and DOE-BES under Award
248 #DE-FG02-99ER45775, with partial instrumentation funding by NSF. GeoSoilEnviroCARS
249 is supported by the National Science Foundation-Earth Sciences (EAR-1128799) and De-
250 partment of Energy-GeoSciences (DE-FG02-94ER14466). The Advanced Photon Source is
251 a U.S. Department of Energy (DOE) Office of Science User Facility operated for the DOE
252 Office of Science by Argonne National Laboratory under Contract #DE-AC02-06CH11357.

253 ¹ D. L. Decker, W. A. Bassett, L. Merrill, H. T. Hall, and J. D. Barnett, Journal of Physical and
254 Chemical Reference Data **1**, 773 (1972).

255 ² R. Boehler, M. Ross, and D. B. Boercker, Physical Review Letters **78**, 4589 (1997).

256 ³ S. N. Vaidya, G. C. Kennedy, P. Physics, and L. Angeles, Journal of Physics and Chemistry of
257 Solids **32**, 951 (1971).

258 ⁴ T. Yagi, Solid State Communications **25**, vi (1978).

- 259 ⁵ A. J. Campbell and D. L. Heinz, *Journal of Physics and Chemistry of Solids* **52**, 495 (1991).
- 260 ⁶ A. Dewaele, A. B. Belonoshko, G. Garbarino, F. Occelli, P. Bouvier, M. Hanfland, and
261 M. Mezouar, *Physical Review B - Condensed Matter and Materials Physics* **85**, 214105 (2012).
- 262 ⁷ D. Walker, L. M. D. Cranswick, P. K. Verma, S. M. Clark, and S. Buhre, *American Mineralogist*
263 **87**, 805 (2002).
- 264 ⁸ A. J. Campbell and D. L. Heinz, *Journal of Geophysical Research* **99**, 11,765 (1994).
- 265 ⁹ A. J. Campbell, L. Danielson, K. Righter, C. T. Seagle, Y. Wang, and V. B. Prakapenka, *Earth
266 and Planetary Science Letters* **286**, 556 (2009).
- 267 ¹⁰ V. B. Prakapenka, a. Kubo, a. Kuznetsov, a. Laskin, O. Shkurikhin, P. Dera, M. L. Rivers, and
268 S. R. Sutton, *High Pressure Research* **28**, 225 (2008).
- 269 ¹¹ Y. Meng, G. Shen, and H. K. Mao, *Journal of physics. Condensed matter : an Institute of
270 Physics journal* **18**, S1097 (2006).
- 271 ¹² A. J. Campbell, C. T. Seagle, D. L. Heinz, G. Shen, and V. B. Prakapenka, *Physics of the
272 Earth and Planetary Interiors* **162**, 119 (2007).
- 273 ¹³ C. Prescher and V. B. Prakapenka, *High Pressure Research* , 1 (2015).
- 274 ¹⁴ K. Takemura and A. Dewaele, *Physical Review B - Condensed Matter and Materials Physics*
275 **78**, 1 (2008).
- 276 ¹⁵ P. I. Dorogokupets and A. R. Oganov, *Physical Review B - Condensed Matter and Materials
277 Physics* **75**, 1 (2007).
- 278 ¹⁶ *See Supplementary Material at [jurlz](#) for the measured pressure-volume-temperature data of KCl
279 from this study.*
- 280 ¹⁷ S. M. Arveson, B. Kiefer, J. Deng, Z. Liu, and K. K. M. Lee, *Physical Review B* **97**, 094103
281 (2018).
- 282 ¹⁸ F. Birch, *J. Geophys. Res.* **83**, 1257 (1978).
- 283 ¹⁹ M. van Thiel, in *Rep. UCRL - 50108* (Lawrence Livermore National Laboratory, Livermore,
284 CA, 1977).